FEM과 BEM을 사용한 소리 굽쇠 분석

장순석, 이제형, 최은영
조선대학교 정보제어계측공학부

Tuning Fork Analysis using FEM and FEM

Soon Suck Jarng, Je Hyeong Lee
Dept. of Information Control & Instrumentation, Chosun University, Korea

Abstract

An unconstrained tuning fork with a 3-D model has been numerically analyzed by Finite Element Method (FEM) and Boundary Element Method (BEM). The first three natural frequencies were calculated by the FEM modal analysis. Then the change of the modal frequencies was examined with the variation of the tuning fork length and width. Analytical model equations were derived from the numerically relating results of the modal frequency-tuning fork length by approximating minimization. Finally the BEM was used for the sound pressure field calculation from the structural displacement data.

1. Introduction

The tuning fork was firstly invented in England by Royal trumpeter John Shore in 1711 [1]. A tuning fork has its natural (modal) frequencies according to its materialistic and structural fabrication. Even though the tuning fork has a long history, its numerical analysis is not well known. Many questions about the tuning fork might be arisen; the variation of the tuning fork length, the effect of the tuning fork width size, the sound pressure intensity around the tuning fork and material aspects etc. This paper answers to those questions. An unconstrained tuning fork with a 3-D model has been numerically analyzed by Finite Element Method (FEM) and Boundary Element Method (BEM). The FEM is used for calculation of modal frequencies and modal shapes (displacements) while the BEM is used for calculation of sound pressure in the 3-D space generated by the tuning fork at the natural frequency. This paper deals with not only the analysis of the tuning fork but also the practical design of the tuning fork.

2. Numerical Methods

2.1 Finite Element Method (FEM)

The following equation (1) is the integral formulation of the FEM elastic equations:

$$\{F\} = [K]\{a\} - \omega^2[M]\{a\} \qquad (1)$$

2.2 Boundary Element Method (BEM)

For sinusoidal steady-state problems, the Helmholtz equation, $\nabla^2\Psi + k^2\Psi = 0$ represents the fluid mechanics. Ψ is the acoustic pressure with time variation, $e^{j\omega t}$, and k(=ω /c) is the wave number. c is the sound speed, 340 [m/sec]. In order to solve the Helmholtz equation in an infinite air media, a solution to the equation must not only satisfy structural surface boundary condition (BC), $\partial\Psi/\partial n = \rho_f \omega^2 a_n$ but also the radiation condition at infinity, $\lim_{|r|\to\infty} \int_S (\partial\Psi/\partial r + jk\Psi)^2 dS = 0$.

$\partial/\partial n$ represents differentiation along the outward normal to the boundary. ρ_f and a_n are the fluid density and the normal displacement on the structural surface. The Helmholtz integral equation derived from Green's second theorem provides such a solution for radiating pressure waves;

$$\int_S \left(\Psi(q)\frac{\partial G_k(p,q)}{\partial n_q} - G_k(p,q)\frac{\partial \Psi(q)}{\partial n_q} \right) dS_q = \beta(p)\ \Psi(p) \qquad (2)$$

where $G_k(p,q) = e^{-jkr}/4\pi r$, $r = |p-q|$

p is any point in either the interior or the exterior and q is the

surface point of integration. β (p) is the exterior solid angle at p

The acoustic pressure for the i^{th} global node, $\Psi(p_i)$, is expressed in discrete form [3]: $(\ 1 \le i \le ng\ )$

$$\beta(p_i)\Psi(p_i) = \int_S \left(\Psi(q)\frac{\partial G_k(p_i,q)}{\partial n_q} - G_k(p_i,q)\frac{\partial \Psi(q)}{\partial n_q} \right) dS_q \qquad (3a)$$

$$= \sum_{m=1}^{nt} \sum_{j=1}^{8} A^i{}_{m,j}\Psi_{m,j} - \rho_f \omega^2 \sum_{m=1}^{nt} \sum_{j=1}^{8} B^j{}_{m,j} a_{m,j} \qquad (3e)$$

where nt is the total number of surface elements and $a_{m,j}$ are three dimensional displacements. When equation (3e) is globally assembled, the discrete Helmholtz equation can be represented as

$$([A] - \beta[I])\{\Psi\} = +\rho_f \omega^2 [B]\{a\} \qquad (4)$$

where [A] and [B] are square matrices of (ng; by ng) size. ng is the total number of surface nodes.

When the impedance matrices of equation (4), [A] and [B], are computed, two types of singularity arise [4]. One is that the Green's function of the equation, $G_k(p_i,q)$, becomes infinite as q approaches to p_i. This problem is solved by mapping such rectangular local coordinates into triangular local coordinates and again into polar local coordinates [5]. The other is that at certain wave number the matrices become ill-conditioned. These wave number are corresponding to eigenvalues of the interior Dirichlet problem [6]. One approach to overcome the matrix singularity is that [A] and [B] of equation (4) are modified to provide a unique solution for the entire frequency range [7-10]. The modified matrix equation referred to as the modified Helmholtz gradient formulation (HGF) [10] is obtained by adding a multiple of an extra integral equation to equation (4).

$$([A] - \beta[I] \oplus \alpha[C])\{\Psi\} = +\rho_f \omega^2 ([B] \oplus \alpha[D])\{a\} \qquad (5)$$

The derivation of the extra matrices [C], [D] are well described by Francis D.T.I. [10].

$$\{\Psi\} = +\rho_f \omega^2 \left(A^{\oplus}\right)^{-1} B^{\oplus}\{a\} \qquad (8)$$

Since the present acoustic vibrator produces displacement data $\{a\}$ at a natural frequency, the surface pressure $\{\Psi\}$ of the tuning fork is calculated from equation (8). Once $\{a\}$ and $\{\Psi\}$ are known, the acoustic pressure in the far field is determined by $\beta(p) = 1$ of equation (2) for given values of surface nodal pressure and surface nodal displacement;

$$\Psi(p_i) = \sum_{m=1}^{nt} \sum_{j=1}^{8} A^i{}_{m,j}\Psi_{m,j} - \rho_f \omega^2 \sum_{m=1}^{nt} \sum_{j=1}^{8} B^i{}_{m,j}\, a_{m,j} \qquad (9)$$

3. Results

The particular structure considered is an unconstrained tuning fork (Fig. 2). The whole tuning fork had been divided into 550 isoparametric elements . Global node numbers are 3934 nodes. Table 1 shows the material properties of the air, steel and aluminum. The first three natural frequencies were calculated from the FEM equation (1) where $\{F\}$=0. In modal analysis $\{a\}$ is an eigenvector and $\lambda = (\omega^2)$ is an eigenvalue.

$$[K]\{a\} = \lambda[M]\{a\} \left(= \omega^2 [M]\{a\}\right) \qquad (10)$$

Fig. 3 shows the modal shape of the tuning fork at 128.4 Hz (1st mode). The length and the width of the tuning fork are 152.4 [mm] and 25.4 [mm]. And the applied material is steel (4130). The green frame is the undeformed shape of the tuning fork while the solid color shows the Von Mises stress (Equation 11) with deformed shape.

$$\sqrt{0.5\left[(\sigma_1 - \sigma_2)^2 + (\sigma_2 - \sigma_3)^2 + (\sigma_3 - \sigma_1)^2\right]} \qquad (11)$$

where $\sigma_1, \sigma_2, \sigma_3$ are stresses in x, y, z coordinates.

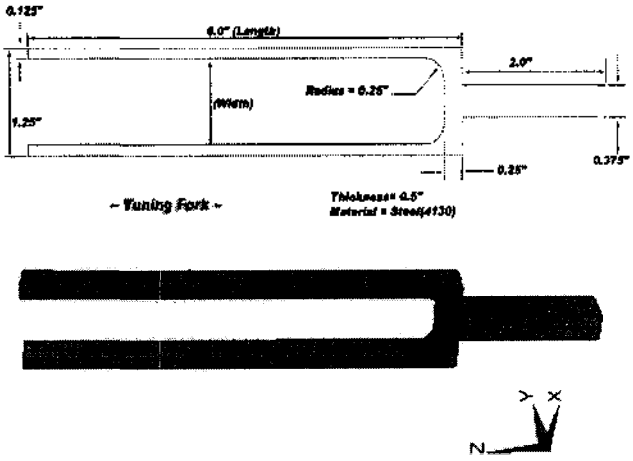

Fig. 2 3D tuning fork dimensions. Elements=550. Nodes=3934

Table 1 Material Properties

	Density (ρ) [Kg/m^3]	Young's Modulus (E) [N/m^2]	Poisson Ratio (V)
Air	1.22	1.411E5	-
Steel	7822.9	2.0684E11	0.30
Aluminum	2703.8	6.9637E10	0.36

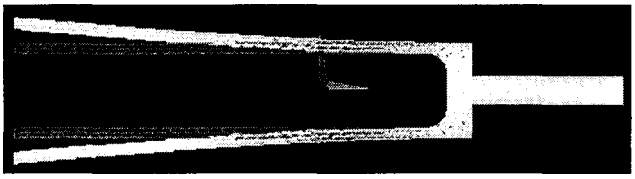

Fig. 3 Modal shape of tuning fork (Color=Von Mises Stress) at 128.4 Hz (1st mode), Length=152.4 [mm], Width=25.4 [mm], Material=Steel(4130)

Then the change of the modal frequencies was calculated with the variation of the tuning fork length and width. Fig. 4 shows the first three modal frequencies as functions of tuning fork length with a constant width. Each symbol indicates different modal frequencies (Circle=1st mode, Diamond=2nd mode, Rectangle=3rd mode). Modal frequencies are exponentially increased with the reduced size of the tuning fork length.

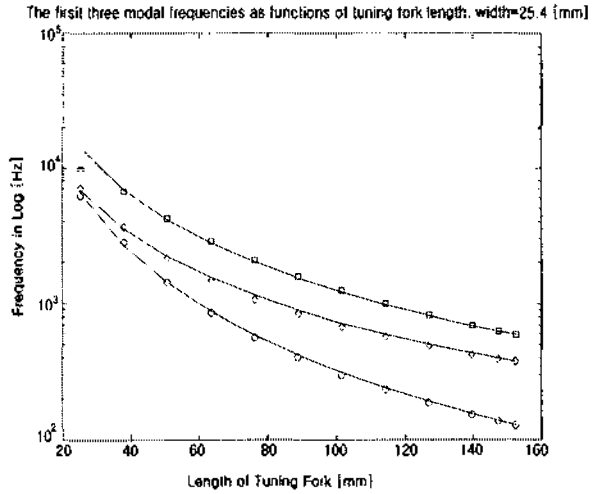

Fig. 4 The first three modal frequencies as functions of tuning fork length.

Circle=1st mode, Diamond=2nd mode, Rectangle=3rd mode.

Analytical model equations were derived from the numerically relating results of the modal frequency-tuning fork length by approximating minimization (Table 2). Solid continuous lines of Fig. 4 were drawn from the analytical model equations for each mode. And Fig 5 shows the comparison in percentage [%] between FEM results and model equations. The most significant difference happened at the 3rd mode with 25.4 [mm] tuning fork length, that is, 44%. But the rests of the results are within 8% differences.

Table 2 Analytical model equations for each tuning fork mode, x [m]

	1st Mode	2nd Mode	3rd Mode
Model Equations	$\frac{2.0859}{x^{2.19}}$	$\frac{17.759}{x^{1.62}}$	$\frac{21.040}{x^{1.77}}$

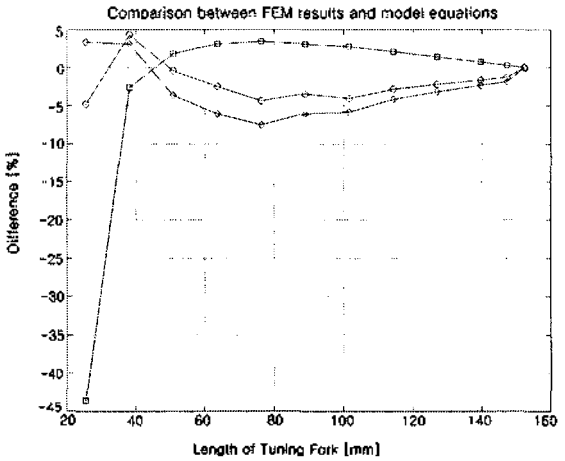

Fig. 5 Comparison in percentage [%] between FEM results and model equations. Circle=1st mode, Diamond=2nd mode, Rectangle=3rd mode.

Table 3 shows that the change of the tuning fork width does not much affect the variation of the modal frequencies. Also Fig. 5 shows that the modal frequencies of the tuning fork remain almost the same as Fig. 4 though the material is changed from steel (continuous line) to aluminum (dashed line). These results show that the length of the tuning fork mainly affects the natural frequencies of the tuning fork as far as metallic materials are used.

Table 3 Modal frequencies with different tuning fork width

Length=152.4 [mm], Material=Steel(4130)

Width	Frequency [Hz]

[mm]	1st mode	2nd mode	3rd mode
50.8	93.5	198.9	525.2
38.1	125.6	339.5	559.5
25.4	128.5	374.1	587.7
12.7	128.6	391.2	576.7
6.3	124.2	395.2	525.5

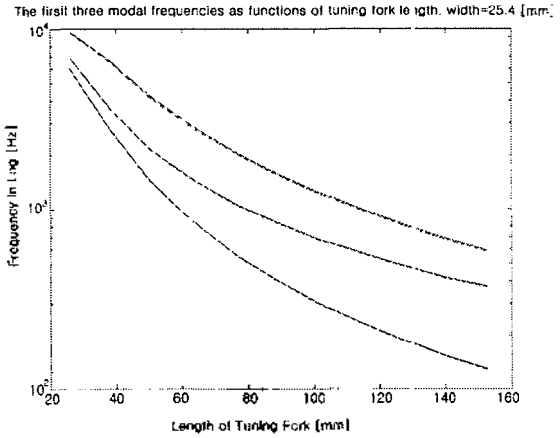

Fig. 6 The first three modal frequencies as functions of tuning fork length as Fig. 4. Continuous Lines=Steel. Dashed Lines=Aluminum

Finally the BEM was used for the sound pressure field calculation from the structural displacement data. From equation (9) the acoustic pressure in the far field is calculated along the circle with the directivity angle ϕ (Fig. 7). The normalized value of the far field pressure is used as the quantitative degree of the directivity. Fig. 7 shows the acoustic pressure directivity pattern at 1 [m] away from the tuning fork at 128.4 Hz (1st mode). Because the modal frequency is low, the directivity pattern is almost omni-directional. And Fig. 8 shows the acoustic pressure radiation pattern of Fig. 7.

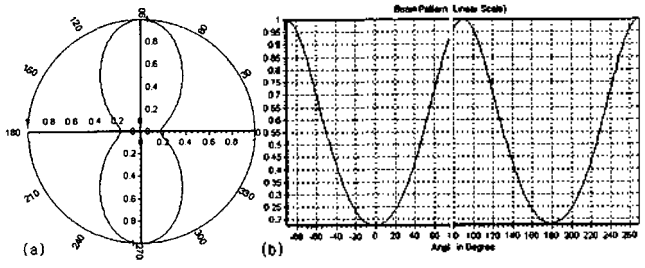

Fig. 7 Acoustic pressure directivity pattern at 1 [m] away from the tuning fork. at 128.4 Hz (1st mode), Length=152.4 [mm], Width=25.4 [mm], Material=Steel(4130)

4. Conclusion

It is concluded that the length of the tuning fork mainly affects the natural frequencies of the tuning fork as far as metallic materials are used. Table 2 showed the designing factor of the tuning fork fabrication. The length of the tuning fork may be changed for a desired first modal frequency such as A pitch (=440Hz) etc. Fig. 8 showed the acoustic pressure radiation pattern generated by the tuning fork. This can be further used for a particular radiation pattern synthesis.

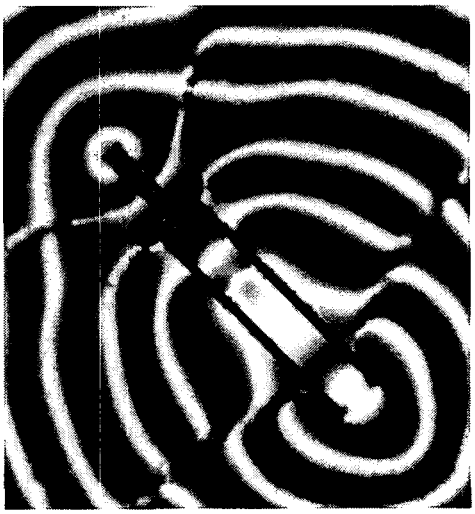

Fig. 8 Acoustic pressure radiation pattern of Fig. 7

References

[1] Alexander J. Ellis."On the History of Musical Pitch," *Journal of the Society of Arts*, March 5, 1880. Reprinted in *Studies in the History of Music Pitch*, Amsterdam: Frits Knuf, p. 44. Ellis measured the pitch of the Streicher fork at A=442.78, 1968.

[2] H. Allik and T.J.R. Hughes, "Finite element method for piezoelectric vibration", Int. J. Numer. Method Eng., Vol. 2, PP:151-157, 1970.

[3] L.G. Copley, "Integral equation method for radiation from vibrating bodies", J. Acoust. Soc. Am. Vol. 41, PP:807-816,